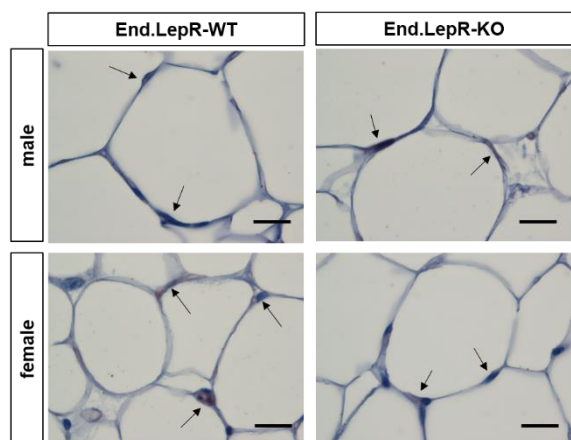
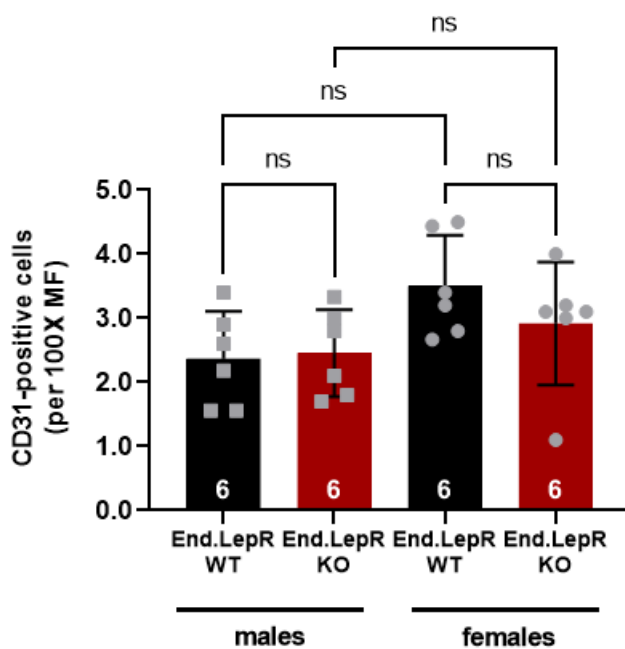


# Suppl. Figure 1

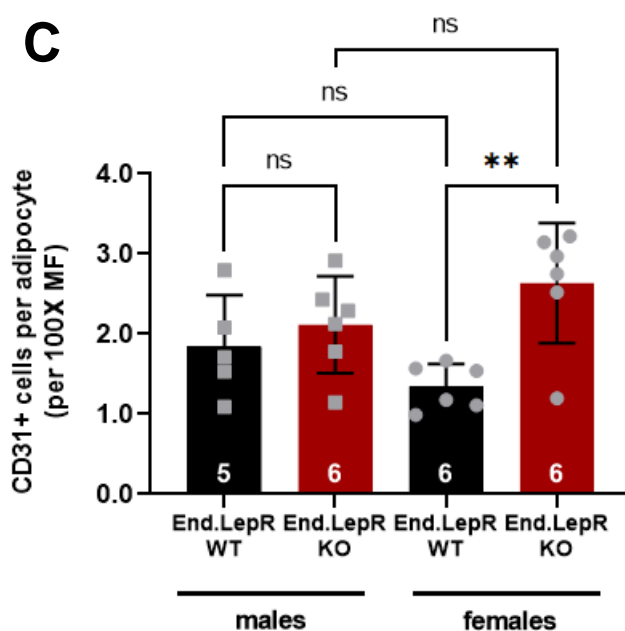
## A



## B



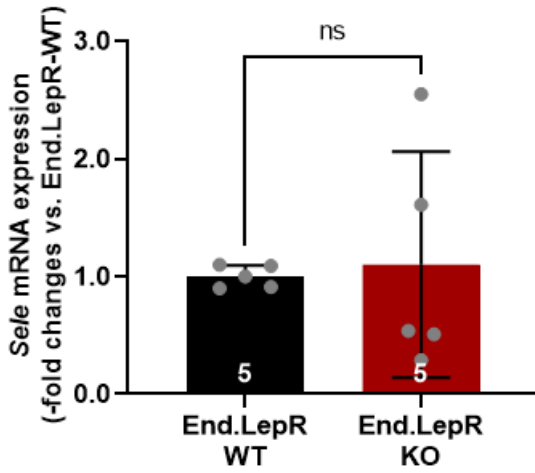
## C



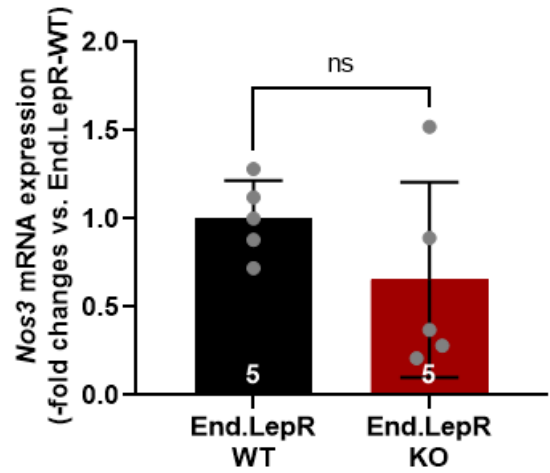
**Supplemental Figure S1. Visceral adipose tissue vascularization.** **A**, Representative microscopic photographs after CD31 immunohistochemical staining of cross-sections through the visceral adipose tissue of male (upper row) and female (lower row) End.LepR-WT and End.LepR-KO mice (n=6 each group) fed 45% high-fat diet for 16 weeks. Scale bars represent 10 μm. Quantitative analysis of the total (**B**) and relative (per adipocyte, **C**) number of CD31-positive cells per microscope field (MF) at 100X magnification. Data were analyzed using Kruskal-Wallis test followed by Dunn' multiple comparisons test. Ns, non-significant.

# Suppl. Figure 2

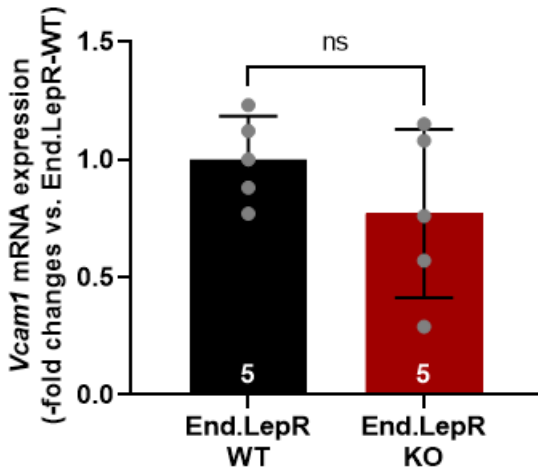
## A



## B

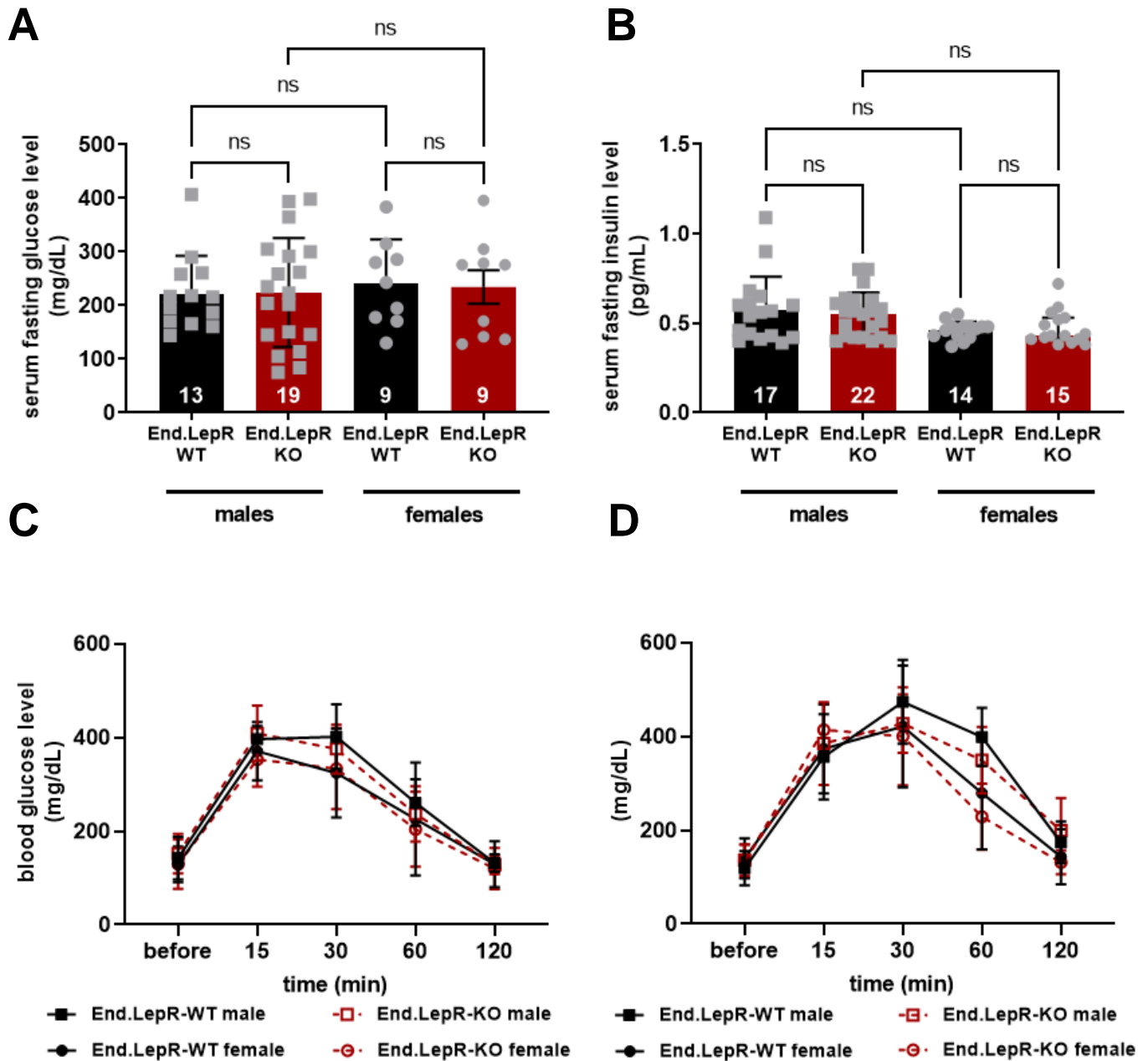


## C



**Supplemental Figure S2. Visceral adipose tissue endothelial gene expression.** Quantitative real-time PCR analysis of primary endothelial cells isolated from visceral adipose tissue of female End.LepR-WT and End.LepR-KO mice (n=5 biological replicates per group) was performed to examine mRNA levels of E-selectin (*Sele*; **A**), endothelial nitric oxide synthase (*Nos3*; **B**) and vascular cell adhesion molecule-1 (*Vcam1*; **C**). Ns, non-significant (Student's t-test).

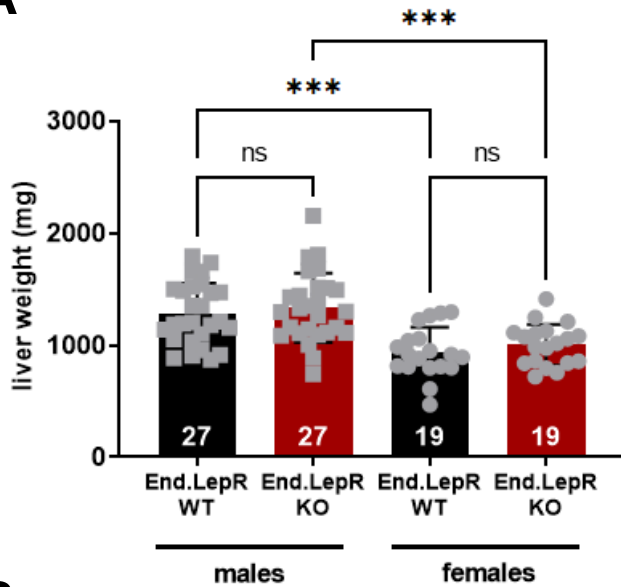
# Suppl. Figure 3



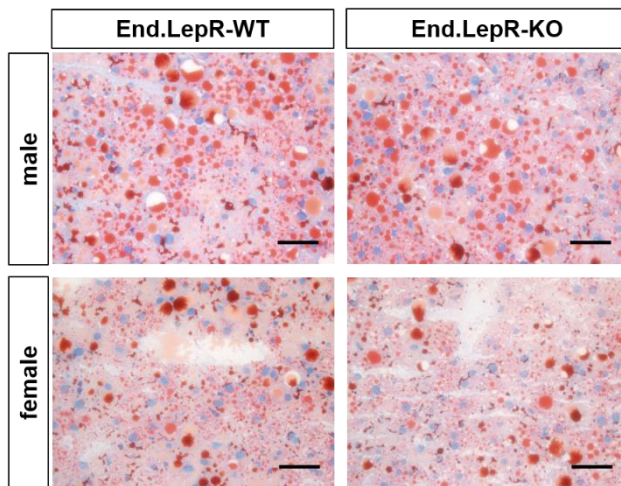
**Supplemental Figure S3. Metabolic serum parameter.** Fasting glucose (A) and insulin (B) levels in serum of male and female End.LepR-WT and End.LepR-KO mice fed high fat diet for 16 weeks. The number of mice examined in each experiment is given in the graph. Data were analyzed using Kruskal-Wallis test, Dunn's multiple comparisons test. ns, non-significant. Glucose tolerance tests were performed in male (n=14 WT and n=15 KO) and female (n=10 WT and n=12 KO) End.LepR-WT and End.LepR-KO mice, fed normal chow (C) or high fat diet (D) for 16 weeks. Mice were fasted for 6 hours followed by intraperitoneal injection of a 20% glucose solution (at a dosage of 2 g/kg body weight in 200  $\mu$ L sterile NaCl). Data were analyzed using Two-Way ANOVA followed by Tukey's multiple comparisons test. Non-significant differences are not shown.

# Suppl. Figure 4

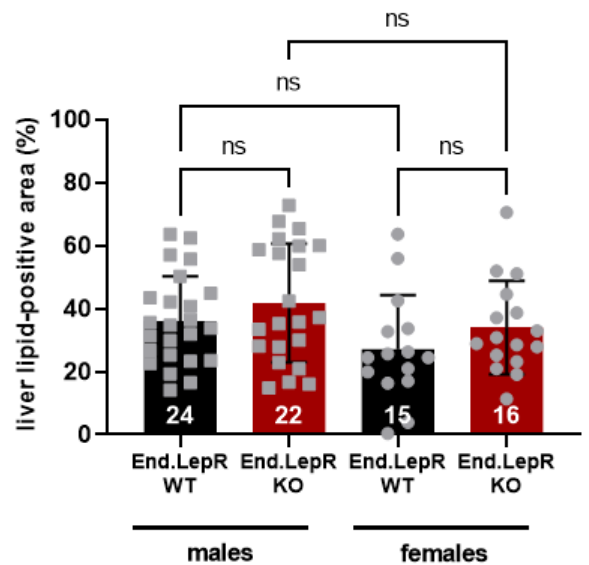
**A**



**B**



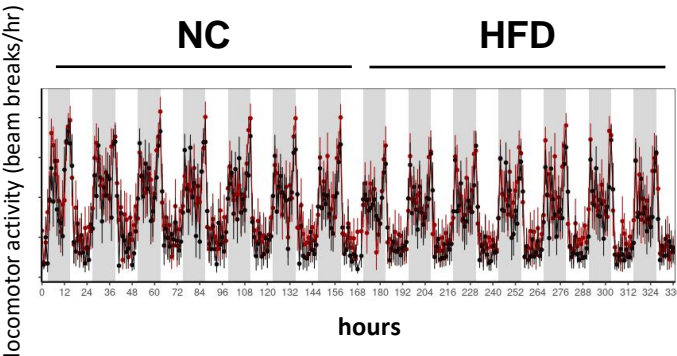
**C**



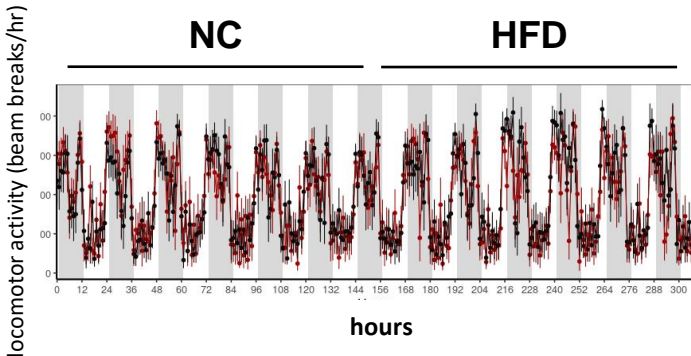
**Supplemental Figure S4. Hepatic lipid accumulation in obesity.** **A**, Liver wet weights of male and female End.LepR-WT and End.LepR-KO mice fed high-fat diet for 16 weeks. Data were analyzed using One-Way ANOVA, Sidak's multiple comparisons test. ns, non-significant. Oil red O staining of cryo-preserved tissue sections through the liver of male and female End.LepR-WT and End.LepR-KO mice. Representative images (**B**) and the results after quantification of the Oil red O-positive area (% of total area at 20X magnification) using ImagePro Plus software (**C**). Scale bars in B represent 20  $\mu$ m. The number of mice examined per group is given in the graphs. Data were analyzed using One-Way ANOVA, Sidak's multiple comparisons test. ns, non-significant.

# Suppl. Figure 5

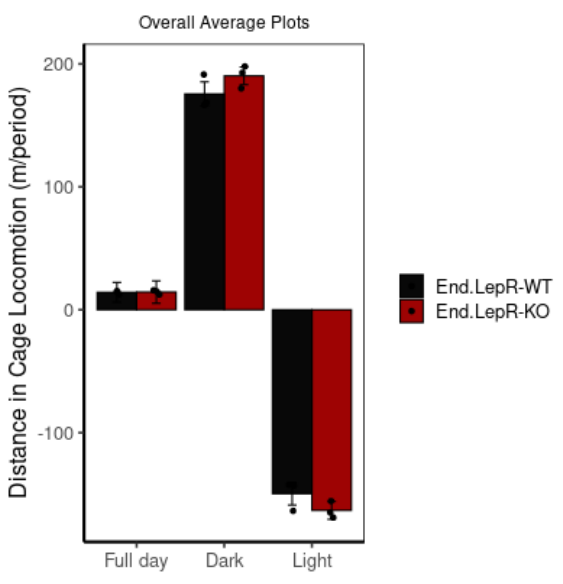
**A**



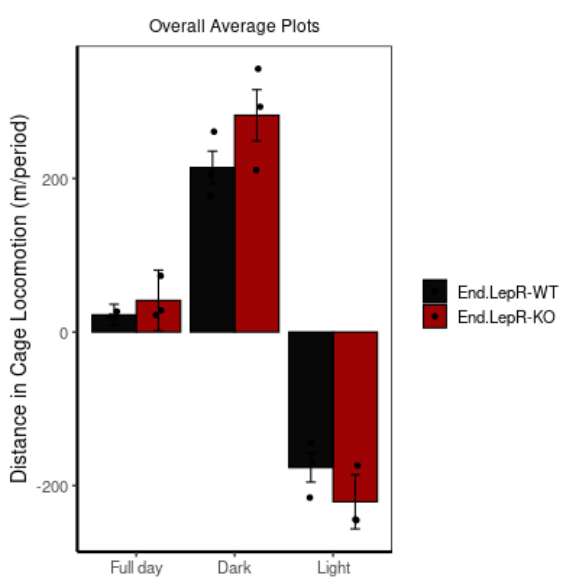
**B**



**C**

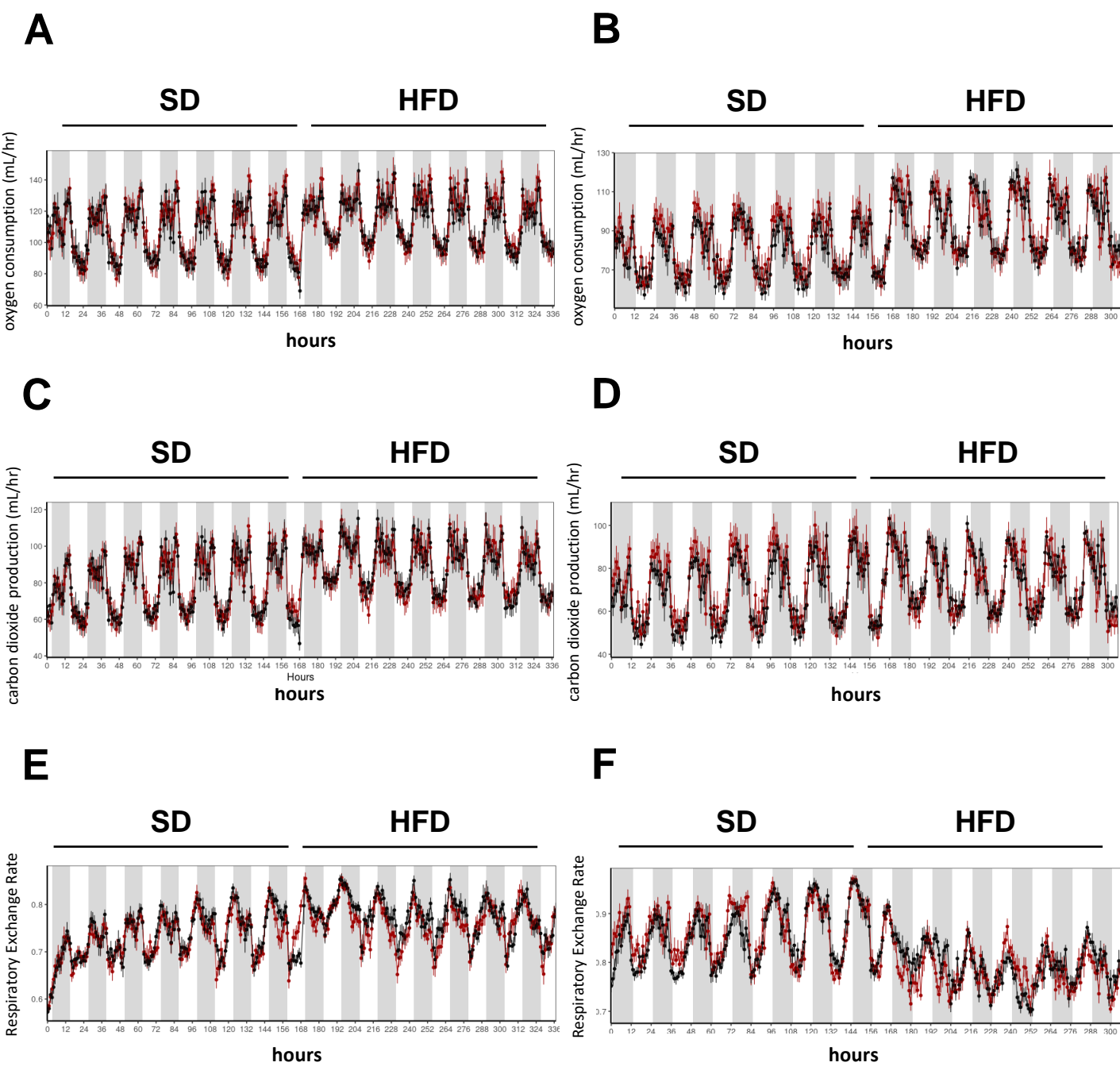


**D**



**Supplemental Figure S5. Physical activity levels.** Locomotor activity of male (A) and female (B) End.LepR-WT (black lines) and End.LepR-KO (red lines) during 7 days on normal chow (NC) followed by a switch to high fat diet (HFD). Distance in cage locomotion of male (C) and female (D) End.LepR-WT and End.LepR-KO mice. Data are shown for the full day or separately for either the dark and the light cycle. N=3 male and female mice, housed in indirect calorimetry cages, were examined genotype.

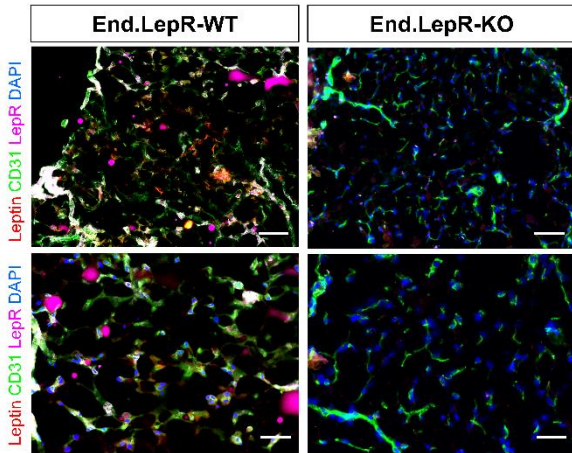
# Suppl. Figure 6



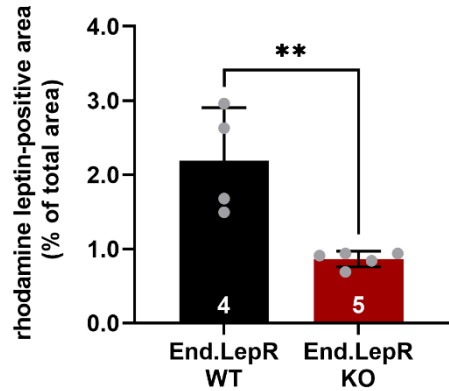
**Supplemental Figure S6. Whole body energy consumption.** Metabolic oxygen consumption (A, B), carbon dioxide release (C, D) and the respiratory exchange ratio (E, F) in male and female End.LepR-WT (black lines) and End.LepR-KO (red lines) mice during 7 days on standard laboratory diet (SD) followed by a switch to high fat diet (HFD) for 7 days are shown. N=3 male and female mice, housed in indirect calorimetry cages, were examined per genotype.

# Suppl. Figure 7

## A



## B

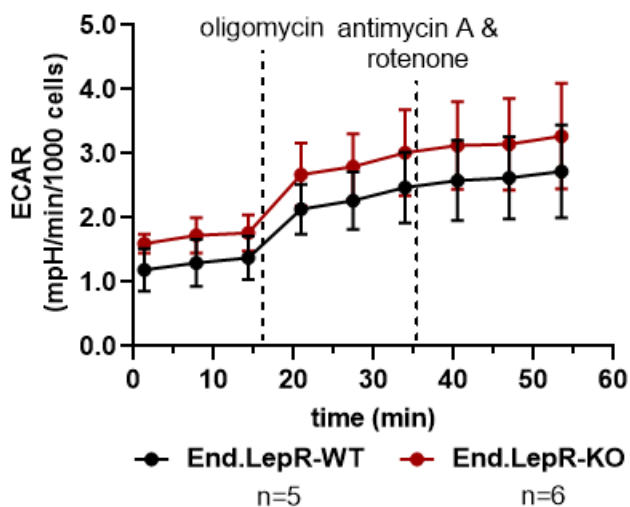


**Supplemental Figure S7. Transport of exogenous recombinant leptin into visceral adipose tissue.** Representative fluorescence microscopy images of cryo-embedded visceral adipose tissue (VAT) sections of End.LepR-WT and End.LepR-KO mice, i.p. injected with rhodamine-labeled leptin (red) and i.c. injected with FITC-labeled lectin to visualize endothelial cells (green), and immunostained for LepR (magenta). DAPI-positive cell nuclei are blue (A). Summary of the quantitative analysis of the rhodamine leptin-positive area per total area of 40X microscopic fields (B). \*\*p=0.004, as determined using Student's t-test. Scale bars in A represent 20 μm (upper row) and 10 μm (lower row).

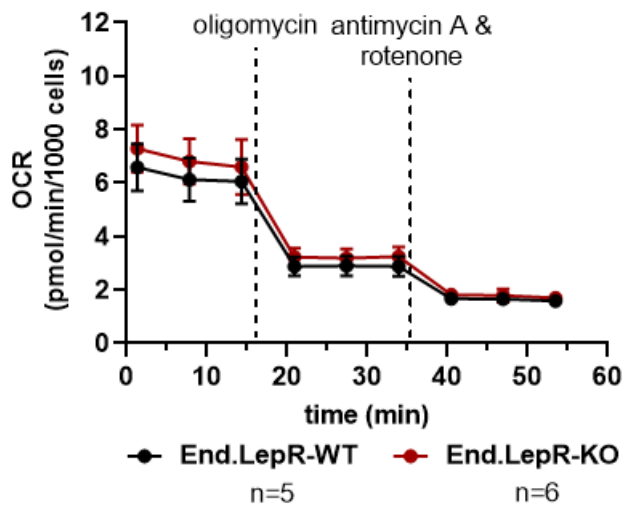


# Suppl. Figure 8

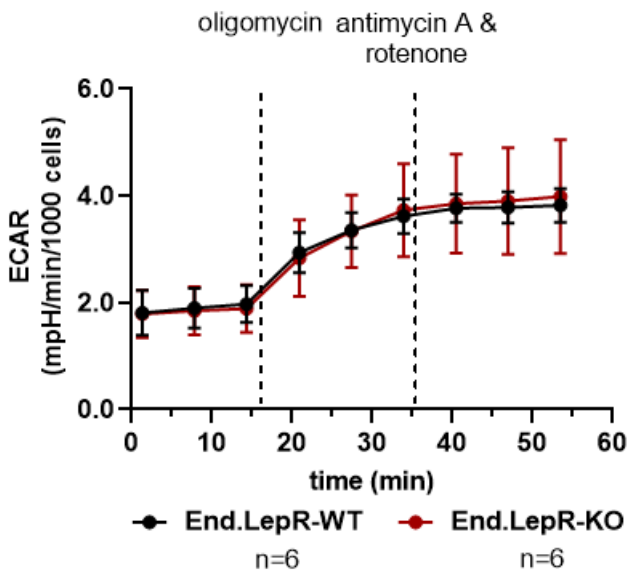
## A



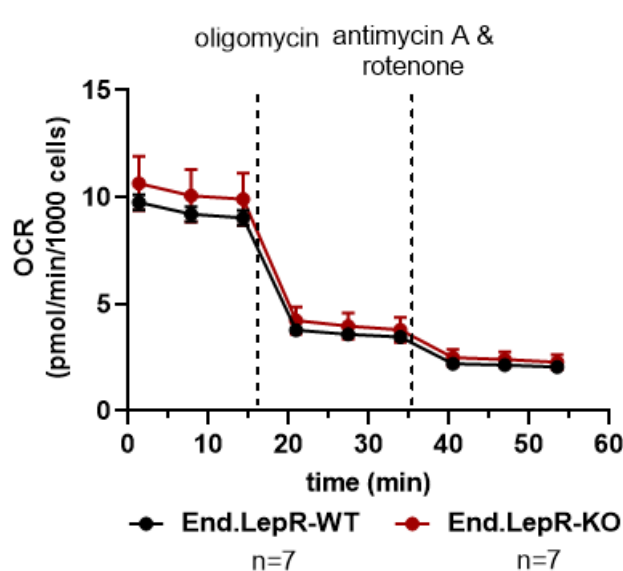
## B



## C



## D



**Supplemental Figure S8. Energy metabolism in primary brain and VAT endothelial cells.** Representative examples of the extracellular acidification rate (ECAR; **A**, **C**) and the oxygen consumption rate (OCR; **B**, **D**) in live primary brain (**A**, **B**) and VAT (**C**, **D**) endothelial cells isolated from female End.LepR-WT and End.LepR-KO mice fed standard diet. Data were analyzed using Two-Way ANOVA, Sidak's multiple comparison tests and did not show significant differences between the two genotypes.